

# Additive-Regulated One-Step Dynamic Spin-Coating for Fabricating High-Performance Perovskite Solar Cells under High Humidity Conditions

Tailin Wang<sup>a</sup>, Teng Zhang<sup>\*a</sup>, Junhua Zhang<sup>a</sup>, Baohua Zhao<sup>a</sup>, Chenhao Song<sup>a</sup>, Hang Yin<sup>b</sup>, Shihui Zhu<sup>a</sup>, Xinyu Sun<sup>a</sup>, Heyuan Liu<sup>a</sup>, Yanli Chen<sup>a</sup>, Xiyou Li<sup>\*a</sup>

<sup>a</sup>School of Materials Science and Engineering, College of Chemistry and Chemical Engineering, China University of Petroleum (East China) Qingdao, 266580, China.

E-mail: [tzhangae@connect.ust.hk](mailto:tzhangae@connect.ust.hk), [xiyouli@upc.edu.cn](mailto:xiyouli@upc.edu.cn)

<sup>b</sup>School of Physics, State Key Laboratory of Crystal Materials, Shandong University, Jinan, Shandong, 250100, P. R. China.



Figure S1. Photographs of the perovskite films prepared under ambient conditions (45% relative humidity) using both spin-coating and dynamic spin-coating methods.

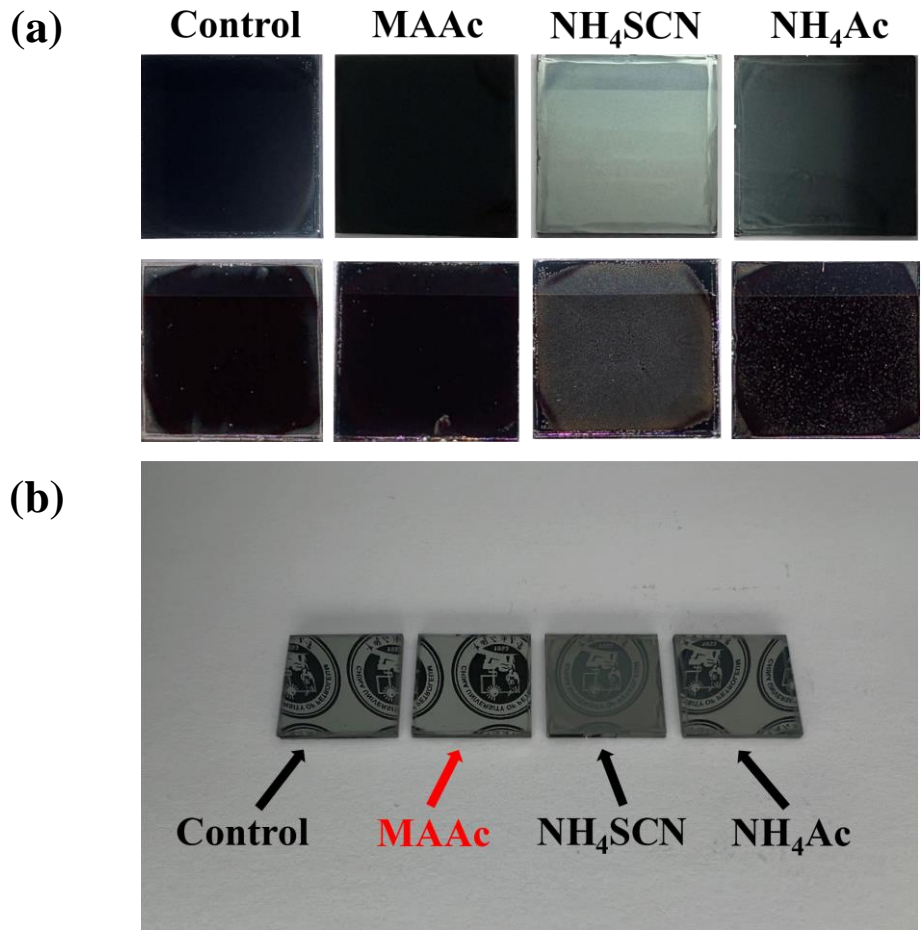


Figure S2. (a) Photographs of the top-view and bottom-view perovskite films prepared without and with the assistance of additives. (b) Mirror-like effect of the prepared perovskite films.

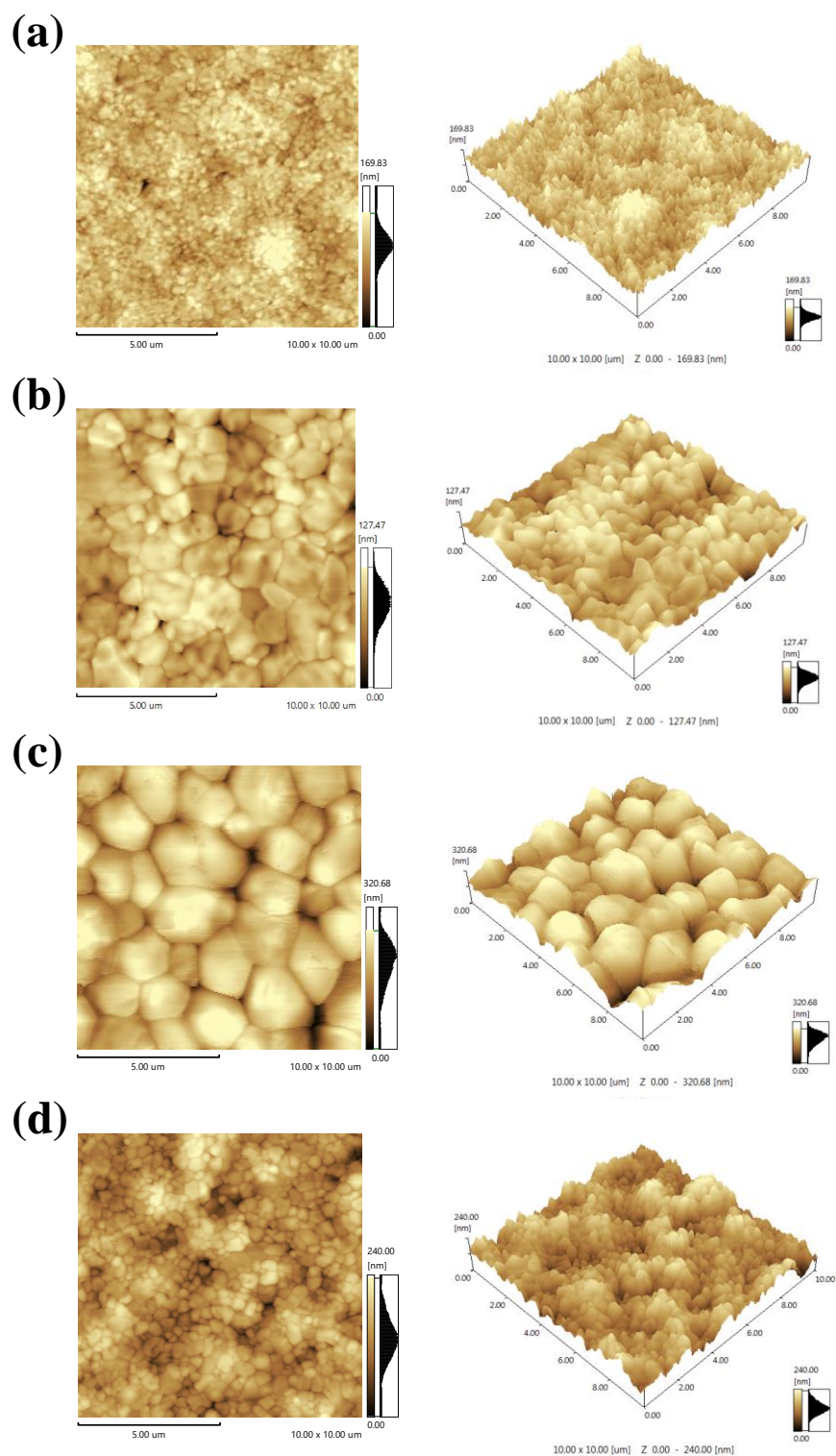


Figure S3. Surface roughness characterization of the perovskite films with the AFM technique, (a) control, (b)MAAc-regulated, (c) NH<sub>4</sub>SCN-regulated, (d) NH<sub>4</sub>Ac-regulated.

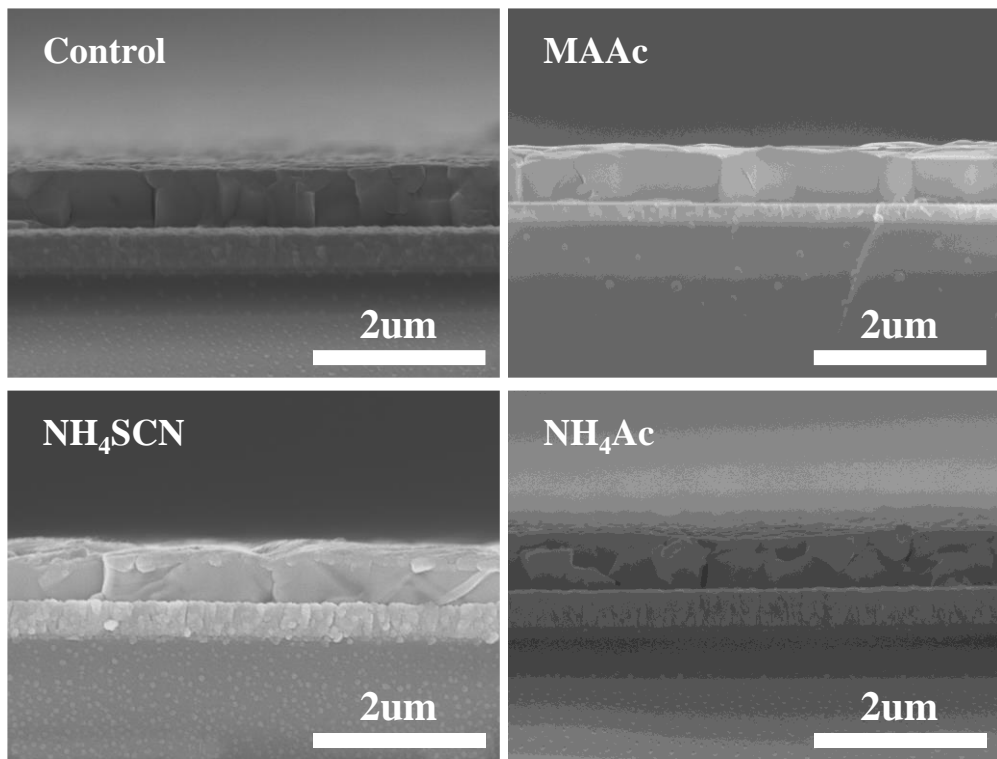


Figure S4. Cross-sectional SEM images of the control and additive-regulated perovskite films, (a) control, (b)MAAc-regulated, (c) NH<sub>4</sub>SCN-regulated, (d) NH<sub>4</sub>Ac-regulated. The scale bar is 2um.

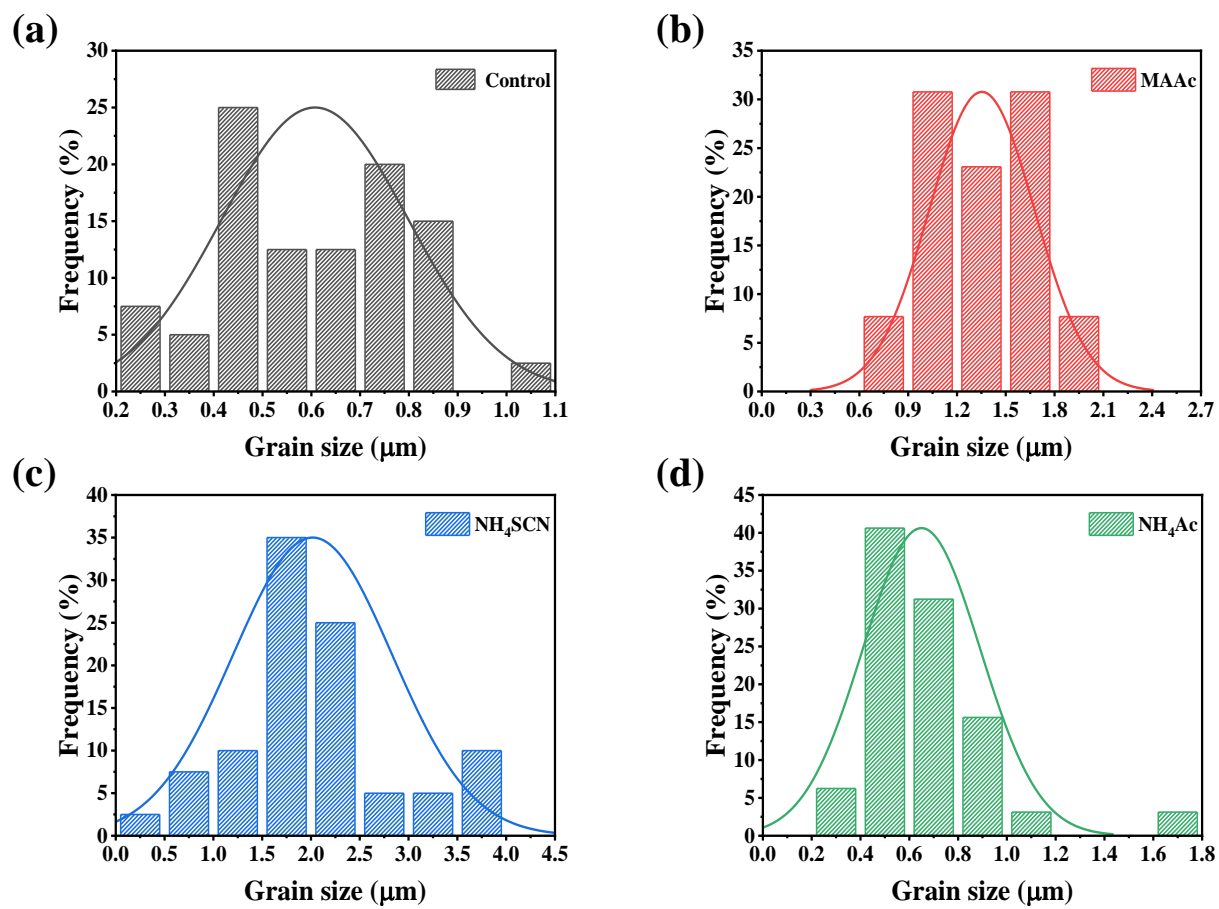


Figure S5. Grain size distribution of the perovskite films calculated from the top-view SEM images.

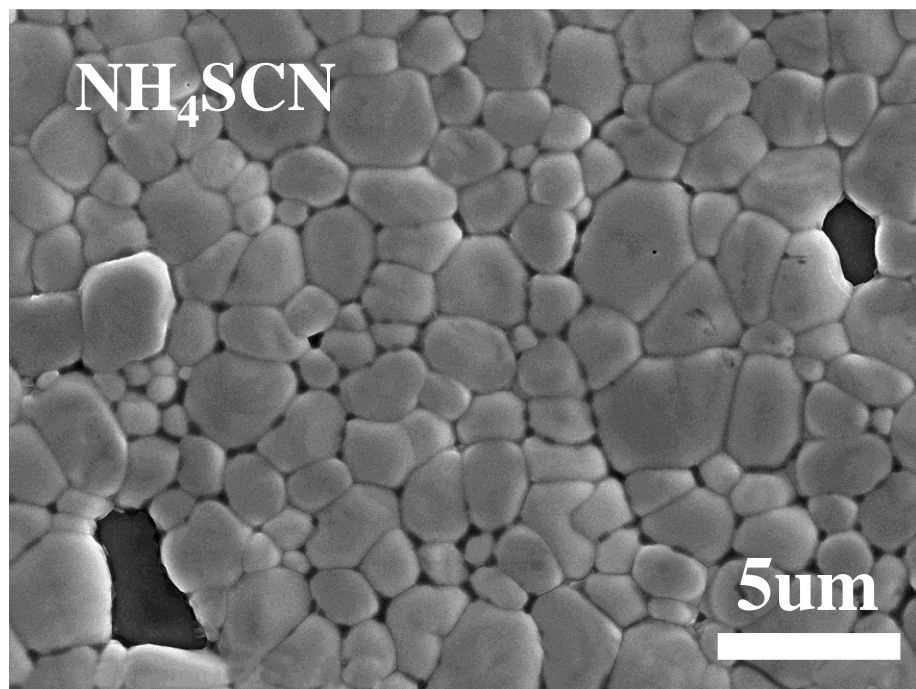


Figure S6. Enlarged top-view SEM image of the NH<sub>4</sub>SCN-regulated perovskite film.

The scale bar is 5um.

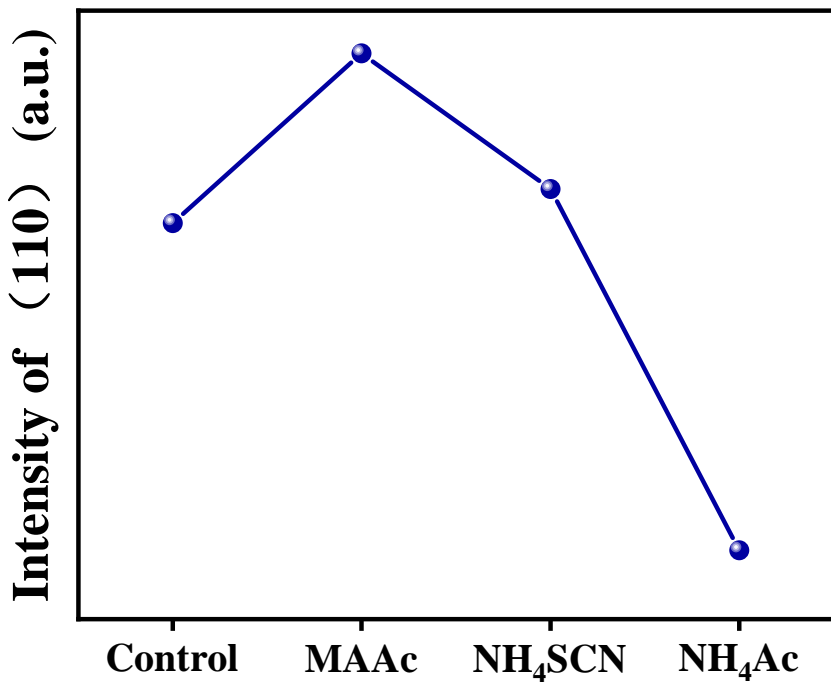


Figure S7. The influence of different additives on the absolute intensity of the (100) peak summarized from Figure 2b.

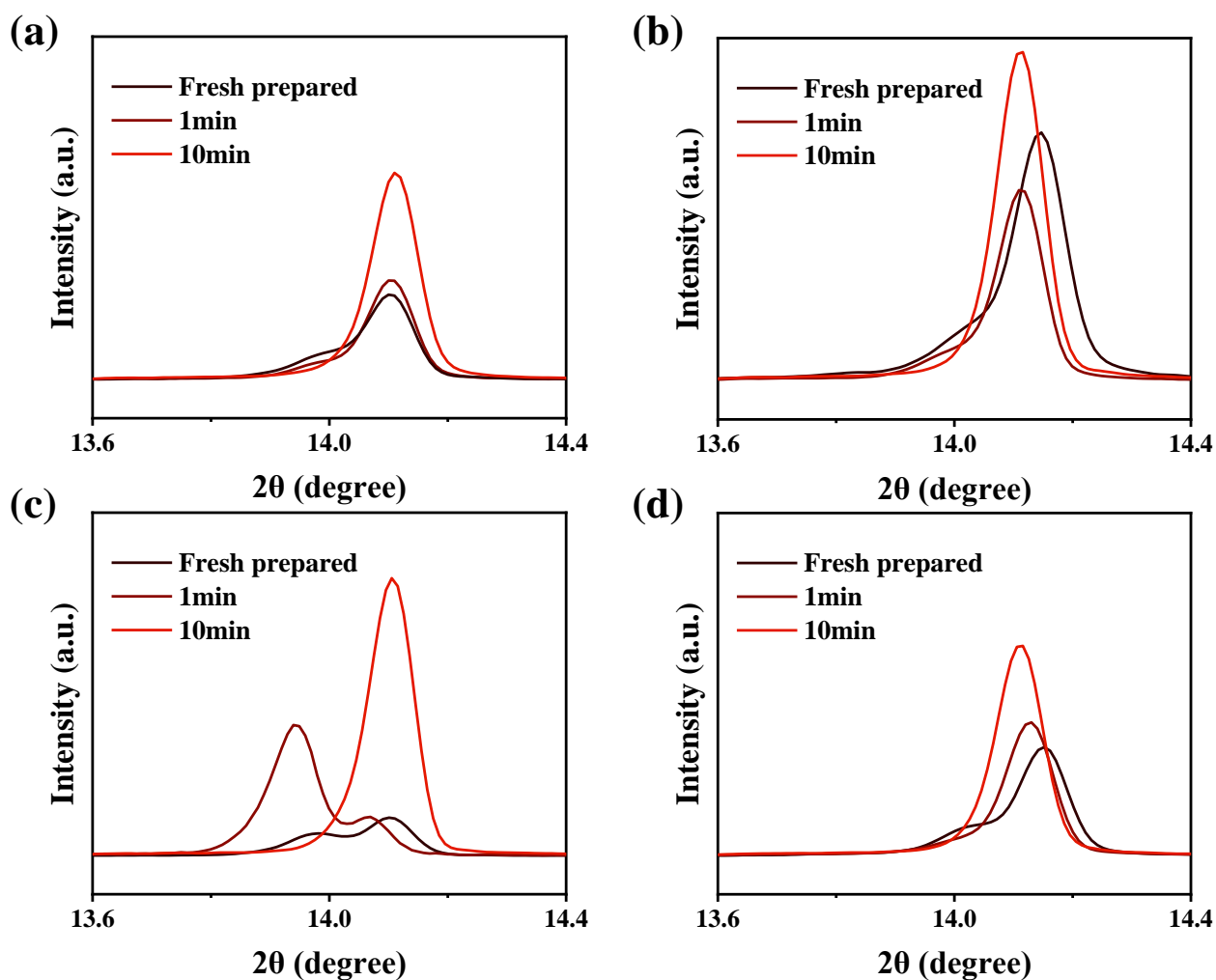


Figure S8. The influence of thermal annealing time on the crystallization process of the fresh prepared films, (a) control, (b)MAAc-regulated, (c) NH<sub>4</sub>SCN-regulated, (d) NH<sub>4</sub>Ac-regulated.

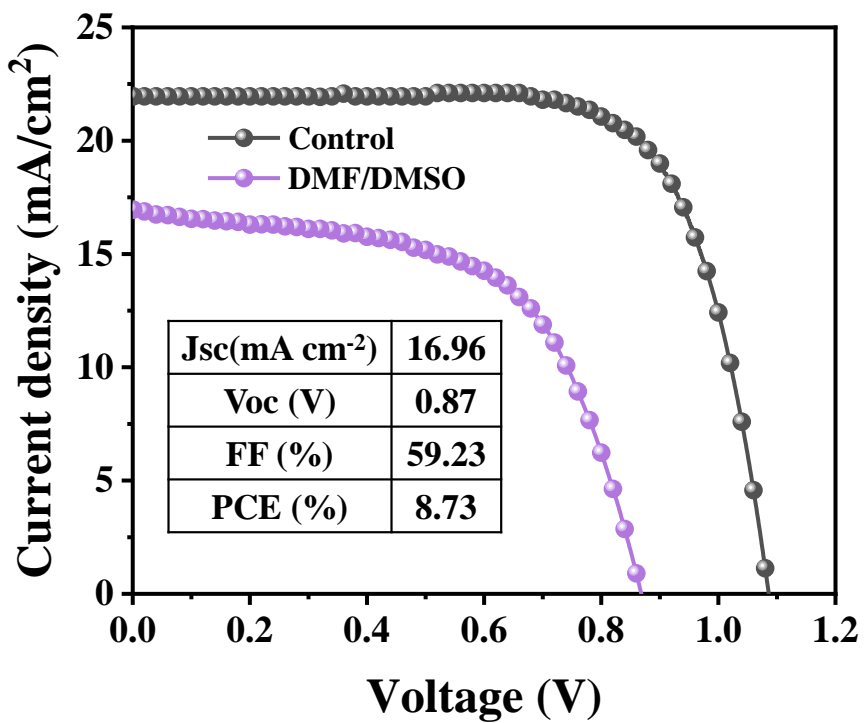


Figure S9.  $J$ - $V$  characteristics of the anitsolvent treated perovskite solar cells deposited in ambient conditions.

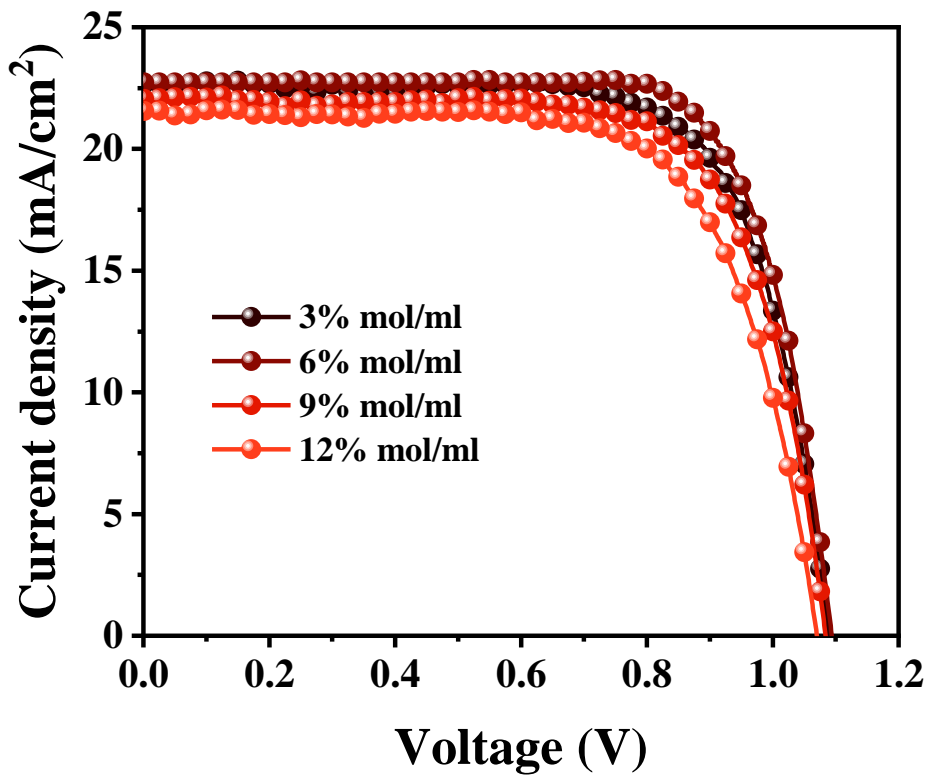


Figure S10. The influence of the MAAc ratio on the *J-V* characterization of the ambient processed PSCs.

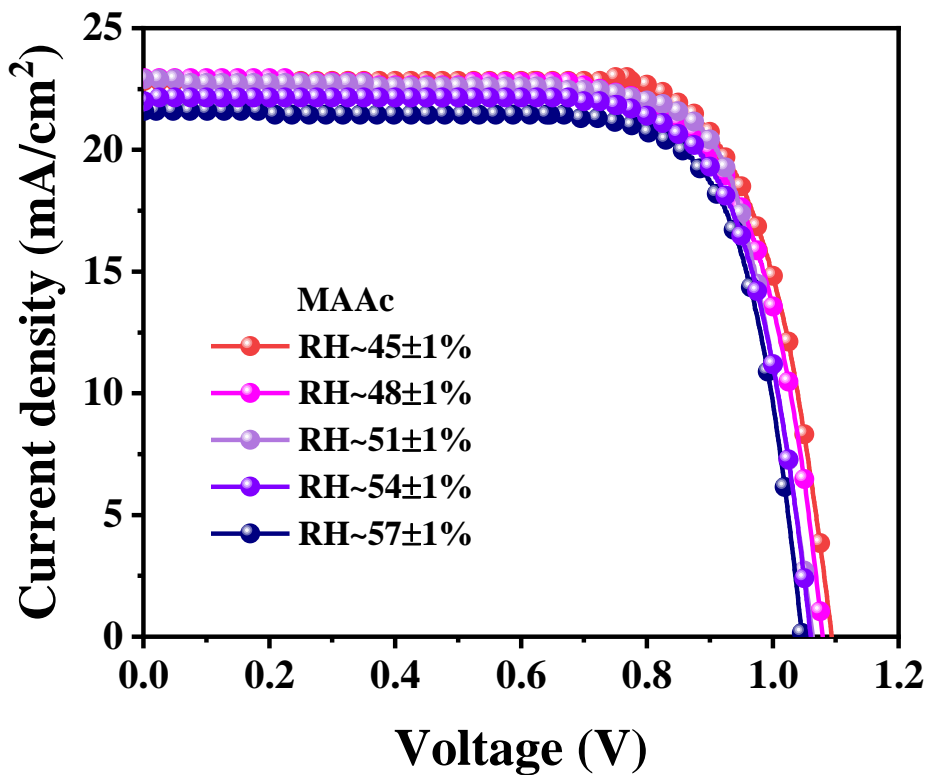


Figure S11. The influence of humidity on the *J-V* characterization of the ambient processed MAAc-regulated PSCs.

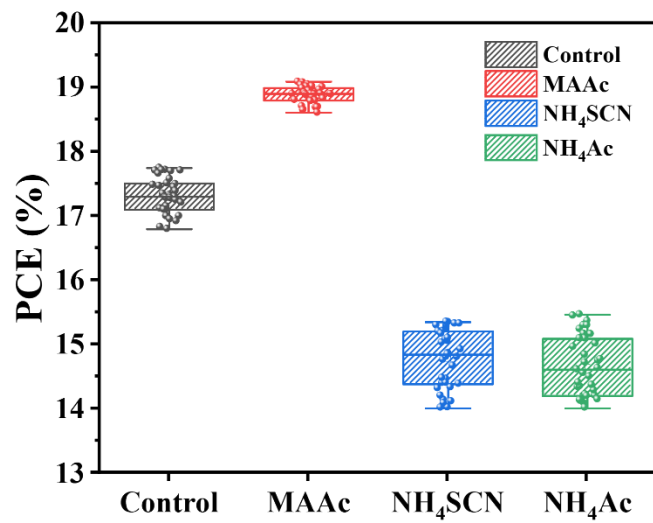


Figure S12. PCE box plots of the control and additive-modified PSCs (35 devices in each condition).

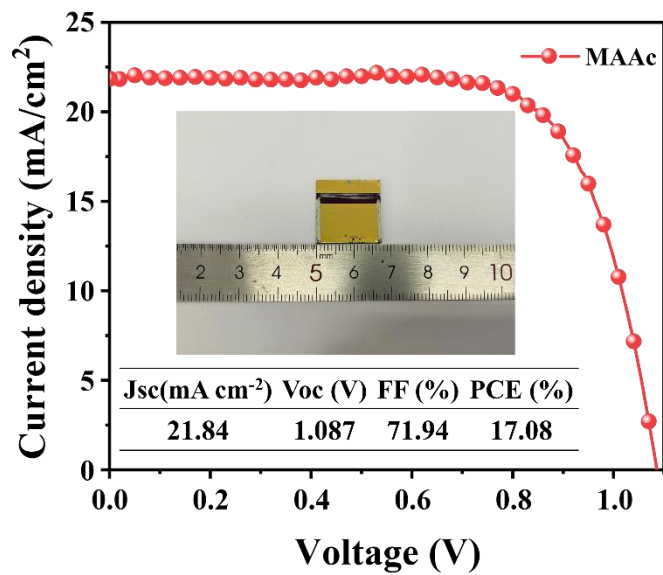


Figure S13.  $J$ - $V$  curves and device parameters for large-scale devices (with an effective area of  $1 \text{ cm}^2$ ).

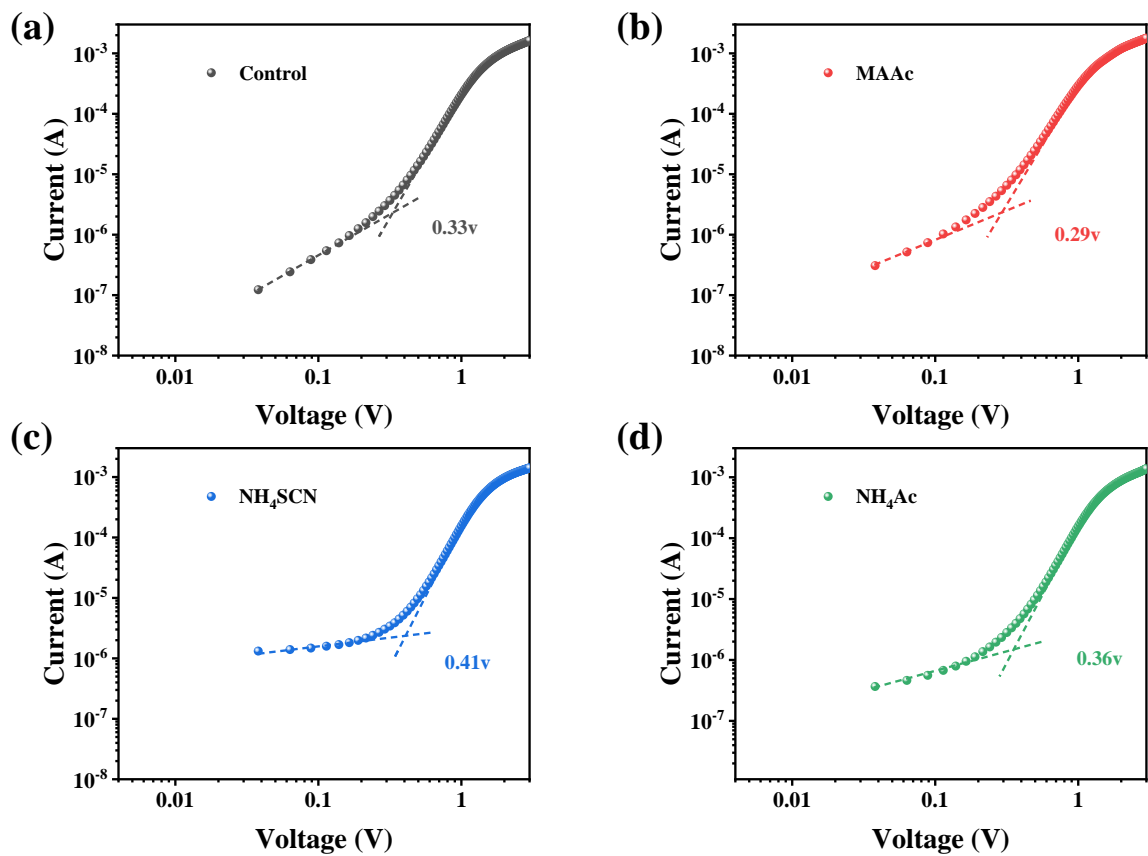


Figure S14. Dark condition  $J$ - $V$  curves of the (a) control, (b)MAAc-regulated, (c) NH<sub>4</sub>SCN-regulated, (d) NH<sub>4</sub>Ac-regulated perovskite films with the device structure of Au/Spiro-OMeTAD/Perovskite (600 nm)/PEDOT:PSS/ITO.

Table S1. The weight loss of the perovskite precursor before and after the TGA characterization.

	25°C (mg)	40°C (mg)	After (mg)	Final percentage (%)
Control	17.3013	9.2680	7.7434	83.55
MAAc	17.3696	9.3363	7.7389	82.89
NH <sub>4</sub> SCN	17.3584	9.3251	7.7389	82.99
NH <sub>4</sub> Ac	17.3591	9.3258	7.7386	82.98

Table S2. Summary of the cell parameters for control and additive-regulated PSCs.

	$J_{sc}$ (mA cm $^{-2}$ )	$V_{oc}$ (V)	FF (%)	PCE (%)
Control	21.954	1.086	74.45	17.75
MAAc	22.736	1.099	76.41	19.09
NH <sub>4</sub> SCN	21.694	0.970	73.09	15.38
NH <sub>4</sub> Ac	21.839	1.007	70.54	15.51

Table S3. A summary PCEs for PSCs prepared by spin coating under the high humidity.

Structures	Methods	Humidity (%)	PCE (%)	Ref.
FTO/TiO <sub>2</sub> /MAPbI <sub>3</sub> /Spiro-OMeTAD/Ag	Spin-coating	50	15.76	[1]
FTO/TiO <sub>2</sub> /MAPbI <sub>3</sub> /Spiro-OMeTAD/Ag	Spin-coating	55	18.2	[2]
ITO/SnO <sub>2</sub> /MAPb(I <sub>1-x</sub> Br <sub>x</sub> ) <sub>3</sub> /Spiro-OMeTAD/Au	Dynamic spin-coating	45-55	19.09	This work
ITO/SnO <sub>2</sub> /MAPbI <sub>3</sub> /Spiro-OMeTAD/Ag	Spin-coating	60	18.34	[3]
ITO/SnO <sub>2</sub> /MAPbI <sub>3</sub> /Spiro-OMeTAD/Ag	Spin-coating	60	19.39	[4]
ITO/Poly-TPD/MAPbI <sub>3</sub> /C <sub>60</sub> /BCP/Ag	Spin-coating	70	18.11	[5]
FTO/NiO/MAPbI <sub>3</sub> /PCBM/Ag	Spin-coating	75	15	[6]
ITO/CPTA/BACl/MAPbI <sub>3</sub> /Spiro-OMeTAD/MoO <sub>3</sub> /Au	Spin-coating	Over 80	20.05	[7]
ITO/SnO <sub>2</sub> /FAPbI <sub>3</sub> /Spiro-OMeTAD/MoO <sub>3</sub> /Au	Spin-coating	70-95	24.1	[8]

Table S4. Concentration dependent cell parameters of the MAAc-regulated PSCs.

Concentration	$J_{sc}$ (mA cm $^{-2}$ )	$V_{oc}$ (V)	FF (%)	PCE (%)
3% mol/ml	22.741	1.089	75.25	18.63
6% mol/ml	22.736	1.099	76.41	19.09
9% mol/ml	22.051	1.083	73.71	17.60
12% mol/ml	21.561	1.075	69.85	16.19

Table S5. Humidity dependent cell parameters of the MAAc-regulated PSCs.

Relative Humidity	$J_{sc}$ (mA cm $^{-2}$ )	$V_{oc}$ (V)	FF (%)	PCE (%)
45±1%	22.736	1.099	76.41	19.09
48±1%	22.872	1.081	75.24	18.60
51±1%	22.702	1.064	75.79	18.31
54±1%	22.552	1.063	75.66	18.14
57±1%	22.363	1.053	75.72	17.83

**Reference:**

- [1] H.S. Ko, J.W. Lee, N.G. Park, 15.76% efficiency perovskite solar cells prepared under high relative humidity: importance of PbI<sub>2</sub> morphology in two-step deposition of CH<sub>3</sub>NH<sub>3</sub>PbI<sub>3</sub>, *J. Mater. Chem. A*, 2015, 3, 8808-8815.
- [2] M.N. Sun, F. Zhang, H.L. Liu, X.G. Li, Y. Xiao, S.R. Wang, Tuning the crystal-growth of perovskite thin-films by adding 2-pyridylthiourea additive for highly efficient and stable solar cells prepared in ambient air, *J. Mater. Chem. A*, 2017, 5, 13448-13456.
- [3] W.T. Wang, J. Sharma, J.W. Chen, C.H. Kao, S.Y. Chen, C.H. Chen, Y.C. Feng, Y. Tai, Nanoparticle-induced fast nucleation of pinhole-free PbI<sub>2</sub> film for ambient-processed highly-efficient perovskite solar cell, *Nano Energy*, 2018, 49, 109-116.
- [4] R. Cheng, C.C. Chung, H. Zhang, Z.W. Zhou, P. Zhai, Y.T. Huang, H. Lee, S.P. Feng, An air knife-assisted recrystallization method for ambient-process planar perovskite solar cells and its dim-light harvesting, *Small*, 2019, 15, 1804465. 12.
- [5] Y.H. Cheng, X.W. Xu, Y.M. Xie, H.W. Li, J. Qing, C.Q. Ma, C.S. Lee, F. So, S.W. Tsang, 18% high-efficiency air-processed perovskite solar cells made in a himid atmosphere of 70% RH, *Solar RRL*, 2017, 1, 1700097.
- [6] J. Troughton, K. Hooper, T.M. Watson, Humidity resistant fabrication of CH<sub>3</sub>NH<sub>3</sub>PbI<sub>3</sub> perovskite solar cells and modules, *Nano Energy*, 2017, 39, 60-68.
- [7] L.F. Chao, Y.D. Xia, B.X. Li, G.C. Xing, Y.H. Chen, W. Huang, Room-temperature molten salt for facile fabrication of efficient and stable perovskite solar cells in ambient air, *Chem*, 2019, 5, 995-1006.
- [8] W. Hui, L.F. Chao, H. Lu, F. Xia, Q. Wei, Z.H. Su, T.T. Niu, L. Tao, B. Du, D.L. Li, Y. Wang, H. Dong, S.W. Zuo, B.X. Li, W. Shi, X.Q. Ran, P. Li, H. Zhang, Z.B. Wu, C.X. Ran, L. Song, G.C. Xing, X.Y. Gao, J. Zhang, Y.D. Xia, Y.H. Chen, W. Huang, Stabilizing black-phase formamidinium perovskite formation at room temperature and high humidity, *Science*, 2021, 371, 1359-1364.